CrossMark

Low-temperature carbon monoxide and propane total oxidation by nanocrystalline cobalt oxides

G. Salek, P. Alphonse, P. Dufour, S. Guillemet-Fritsch, C. Tenailleau*

Centre Interuniversitaire de Recherche et d'Ingénierie des MATériaux (CIRIMAT), UMR CNRS 5085, Université de Toulouse – UPS, 118 route de Narbonne, 31062 Toulouse cedex 09, France

ABSTRACT

Pure CoO(OH), with intra particulate porosity up to 76%, was synthesized by an innovative aqueous precipitation method, starting either from nitrate or sulfate salts. Microstructural and chemical properties were characterized by powder X-ray diffraction (XRD), thermogravimetry (TG) and differential scanning calorimetry (DSC), scanning electron microscopy (SEM) and high-resolution transmission electron microscopy (HRTEM). The primary particles (10–15 nm) are self-organized in monolayer building hexagonal nano-platelets (50–200 nm) which are arranged randomly creating large pores.

CoO(OH) was converted in Co_3O_4 by heating in air at 250 °C. This treatment did not modify the porosity but increased the specific surface area, which became close to $100\,m^2/g$. The catalytic activity for CO and C_3H_8 total oxidation was better for Co_3O_4 than for CoO(OH). Besides, at high conversion rate, catalysts prepared from sulfate precursor showed a superior activity for C_3H_8 oxidation than those prepared from nitrate. This effect can be explained by the improved accessibility of reactants to the surface of the catalysts which exhibit a larger porosity. To our knowledge, the activity values presented here are the highest reported in literature for C_3H_8 total oxidation.

© 2013 Elsevier B.V. All rights reserved.

1. Introduction

Precious metal catalysts (Pt, Pd, Rh) have been commonly used in automotive and industrial catalytic converters since the 1980s for the total oxidation of CO and other exhaust gases [1,2]. Despite their high efficiency, their excessive cost and limited availability drives research scientists to explore alternative catalysts. Many investigations have demonstrated that single and mixed transition metal oxides could have an excellent catalytic activity on total oxidation of CO and hydrocarbons [3–6]. Among these oxides, Co_3O_4 has been reported to be the best catalyst for oxidation of CO [5–11] and total oxidation of hydrocarbons [12–14]. However, Co_3O_4 is not suitable for high temperature applications such as automotive converters because it loses oxygen above 900 °C [15] to form less active CoO or inactive $CoAl_2O_4$ spinel when it is supported on alumina [16]. Nevertheless, it still remains a perfect candidate for low temperature applications like VOC removal.

Synthesis of Co_3O_4 has been widely studied either by dry or wet methods. The wet methods used for preparing cobalt oxide include combustion [17], sol–gel [18], precipitation and coprecipitation [19–22], hydrothermal [23–25] and solvothermal [26].

Recently we reported a new synthesis process of Co–Mn spinel oxides [27] based on the precipitation at room temperature of nanocrystalline particles with a narrow size distribution, without using any polymeric agent. This low cost innovative process does not require any organic reactant and can be easily extended to large-scale production.

We used this new process for the synthesis of nanocrystalline CoO(OH). This oxyhydroxide was converted in Co_3O_4 by heating in air. We present here the detailed materials characterizations and the study of their catalytic activity, for CO and C_3H_8 total oxidations.

2. Experimental

2.1. Materials synthesis

Cobalt oxyhydroxide CoO(OH) was prepared by following our method described in a previous paper [27]. Co_3O_4 was obtained after calcination of CoO(OH) in air.

Briefly, a solution of metallic salts was prepared by dissolving cobalt sulfate or cobalt nitrate (0.03 mol, 100 mL) in distilled water. Then, this solution was rapidly poured (5.5 L/s) into a LiOH solution (0.1 mol, 1400 mL) where the pH was kept at a constant value (12 ± 0.1) to obtain a homogenous precipitate. The precipitate was left under constant stirring for 30 min. The color then gradually changed from blue to brown which characterized the formation of

* Corresponding author. Tel.: +33 0561556283.
E-mail address: tenailleau@chimie.ups-tlse.fr (C. Tenailleau).

$Co(OH)_2$. The precipitate was washed until the conductivity of wash water was less than 10 μS/cm. Then, the wet hydroxide was dried at room temperature and CoOOH was formed. In the following, the ND and SD abbreviations will refer to the dry samples prepared from the nitrate and sulfate precursors, respectively.

2.2. Catalysts characterization

Residual lithium and sulfur contents were determined in the samples by Inductively Coupled Plasma Atomic Emission Spectroscopy (ICP-AES) using a Jobin Yvon (JY 2000) analyzer. X-ray Diffraction (XRD) measurements at room temperature were recorded on a Bruker D4-ENDEAVOR diffractometer, in the Bragg–Brentano geometry, using the Cu Kα radiation (40 kV, 40 mA). Diffraction intensities were measured by scanning from 10 to 100° (2θ) with a step size of 0.02° (2θ). A quantitative estimation of the cell parameters and peak broadening was performed by profile fitting of the whole XRD patterns using the Fityk software [28]. An example of fitting is given in online resource 1. Peak profiles were modeled by a pseudo-Voigt function. Refined parameters included the zero shift (2θ), background, unit cell parameters and peak shapes. The refined FWHM (full-width at half-maximum) of the lines was used to compute, by the Scherrer's equation, the average crystallite size. The instrumental broadening contribution was evaluated by using a standard sample of α-alumina.

To study the crystallographic phase transformation with temperature an Anton Paar HTK1200 N high-temperature chamber fitted on a Bruker D8-Advance diffractometer in the Bragg–Brentano geometry was used. The temperature was increased by steps of 25 °C (heating rate of 0.5 °C/min) in the range 100–400 °C. The temperature was kept constant during each pattern acquisition.

Scanning electron microscopy (SEM) images were performed, on a JEOL JSM-6700F instrument while high resolution transmission electron microscopy (HR-TEM) observations were done on a JEOL 2100F instrument at 200 kV, both equipped with a Field Emission Gun (FEG). Samples were prepared by putting a drop of an ethanol suspension of particles either on a glass substrate (SEM) or on a carbon-coated Cu grid (TEM).

Thermogravimetric/differential scanning calorimetry (TGA/DSC) analyses were carried out on a Mettler-Toledo TGA-DSC1 device using aluminum crucibles. Experiments were performed with 20% O_2 in Ar dynamic atmosphere (flow rate of 50 cm³/min) using a heating ramp of 5 °C/min from room temperature to 600 °C.

Specific surface area and pore size distribution were calculated from nitrogen adsorption–desorption isotherms collected at 77 K, using an adsorption analyzer Micromeritics Tristar II 3020. The specific surface areas were computed from adsorption isotherms, using the Brunauer–Emmett–Teller (BET) method [29]. The pore size distributions (PSD) were computed from desorption isotherms by the Non Local Density Functional Theory (NLDFT) method [30] (with Quantachrome Autosorb-1 software). Pore volume (P_v) was calculated from the adsorbed volume (V_a) at a relative pressure of 0.995 by:

$$P_v = V_a \times \left(\frac{N_2 \text{ gas density}}{N_2 \text{ liquid density}} \right) = 0.00155 \, V_a$$

Each sample was degassed at 150 °C overnight (∼16 h) prior to analysis in order to remove the species adsorbed on the surface.

2.3. Determination of catalytic activity

These tests were performed in a differential, tubular, fixed bed flow reactor, at ambient pressure, with a residence time ≈0.03 s (catalyst mass = 0.050 g, volumetric flow rate = 1.63 cm³ s⁻¹). Reactants were dosed by mass flow controllers (Brooks 5850). The
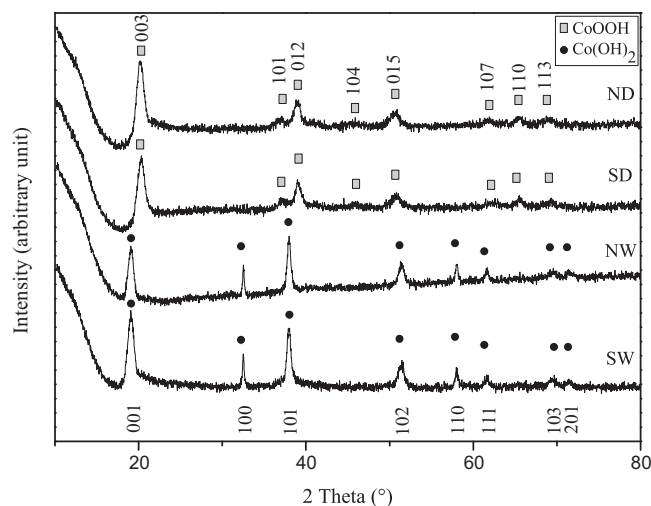
Fig. 1. XRD patterns of SD and ND samples. Bragg peak indices are indicated for each structure: trigonal with the *P3m1* space group for $Co(OH)_2$ and trigonal with the *R-3m* space group for $CoO(OH)$.

catalyst temperature was controlled by a K-type thermocouple positioned inside the catalyst bed. For CO oxidation the temperature range was 30–200 °C and the inlet gas composition was 0.8% CO + 20% O_2 in Ar. For C_3H_8 oxidation the temperature range was 30–300 °C and the inlet gas composition was 0.4% C_3H_8 + 20% O_2 in Ar. The catalyst temperature was increased at a heating rate of 150 °C/h during the CO oxidation and 200 °C/h during the propane oxidation.

The gas phase composition during the tests was monitored by mass spectrometry (HPR20-QIC from Hiden Analytical). Unless otherwise specified, the catalysts were first pretreated with 20% O_2 in Ar for 60 min. To study the catalytic activity of $CoO(OH)$ the thermal treatment temperature was either 140 or 180 °C; for Co_3O_4 the temperature was either 250 or 300 °C.

3. Results and discussion

3.1. Elemental analysis

The lithium residual content in our materials, determined by ICP, was 32 ± 2 ppm for SD and 33 ± 2 ppm for ND. These values are considered to be insignificant to have a measurable effect on the microstructure or catalytic activity.

3.2. X-ray diffraction study

Fig. 1 shows the room temperature XRD patterns of wet sample SW (sulfate precursor), NW (nitrate precursor) and SD and ND samples. Wet samples patterns show only the lines of cobalt β-hydroxide $Co(OH)_2$ which has a trigonal structure (hexagonal lattice) with the *P-3m1* space group (no. 164). Cell parameters and FWHM were obtained from profile fitting of the whole XRD patterns. The data are reported in Table 1. Cell parameters are close to those reported in literature ($a = 0.317$ and $c = 0.464$ nm [JCPDS card 01-074-1057]). A significant difference between the 001 and 100 peak widths are observed, which indicates an anisotropy in the crystallites shapes.

XRD patterns of dried samples show that only the oxyhydroxide $CoO(OH)$ phase is formed. This compound crystallizes with a trigonal symmetry (hexagonal lattice) and the *R-3m* space group (no. 166). Cell parameters and FWHM obtained from profile fitting are also reported in Table 1. The *a* cell parameter, determined after refinement, is close to the value reported in literature whereas *c* is